

# The testing of an evacuated tubular collector with a heat pipe using the Fourier frequency domain

W. KAMMINGA

Department of Applied Physics, University of Groningen, 9747 AG Groningen, The Netherlands

(Received 8 January 1985)

**Abstract**—An outdoor method for the testing of an evacuated tubular collector with a heat pipe under a variable insolation has been described. Based on a heat balance of the collector defined in the Fourier frequency domain, a set of equations corresponding to selective values of the Fourier variable can be formulated. The main collector parameters such as the absorptance–transmittance product, the heat loss resistance and the efficiency factor, follow from a least-square approximation. At least two series of experimental measurements with a different fluid inlet temperature are required.

## 1. INTRODUCTION

IN A PREVIOUS paper [1] the author treated a test method for the conventional flat plate solar collector under variable weather conditions. The collector characteristics were simultaneously solved from a set of algebraic equations by a least-square method. These equations defined in the Fourier frequency domain, followed from a heat balance of the collector, relating generalized expressions of the useful energy, the insolation and the heat losses.

A similar approach will be applied to evacuated tubular collectors, in which a heat pipe transports the heat between the absorber and the condenser. Particularly, for this type of collector, the method can be a valuable addition of existing collector test methods. Because of the specific property of a different heat resistance for the two opposite directions of the heat flow within the heat pipe (diode-effect), the heat loss resistance cannot be determined by the well-known zero-insolation test, in this case. The main collector characteristics of the heat pipe collector are found to be the absorptance–transmittance product,  $\alpha\tau$ , the heat loss resistance,  $R_L$ , and the efficiency factor,  $F'$ . In comparison with the flat plate collector having for  $F'$  a value of approx. 1, the last mentioned factor is of importance in the case of a heat pipe collector. As a result of the non-negligible value of the heat resistance of the fluid layer of the condenser in the heat pipe,  $R_{pc}$ , the efficiency factor considerably differs from 1, in this case.

In practice, the test method is very similar to the case of the flat plate collectors, described in [1]. Because of its sensitivity to errors only a small series of selected values of the Fourier variable is appropriate to derive reliable equations. In order to deal with optimum effects of  $R_{pc}$ , the selection has to be extended with some different values of the Fourier variable.

The test method will be illustrated by the application to the Philips ETC-VTR 141 collector. It will be shown that two series of experimental measurements made by different fluid inlet temperatures are sufficient to determine the collector characteristics.

## 2. THE TEST METHOD FOR A HEAT PIPE COLLECTOR

A detailed description of the theoretical model and the practical application of the test method to the conventional flat plate collector has been given in [1]. In the case of an evacuated tubular collector with a heat pipe, the model can be derived by the same reasonings and the collectors are tested on exactly the same installation. For this reason, only the essential parts describing the test method with a special emphasis on the application to the heat pipe collector will be treated in this chapter.

Representing the collector by a four-node model (see Fig. 1) the temperatures of the glass envelope, the absorber, the condenser and the fluid satisfy, respectively, the time-dependent differential equations

$$C_g \frac{\partial T_g}{\partial t} = \frac{T_a - T_g}{R_{ag}} + \frac{T_p - T_g}{R_{pg}} \quad (1)$$

$$C_p \frac{\partial T_p}{\partial t} = \frac{T_g - T_p}{R_{pg}} + \frac{T_c - T_p}{R_{pc}} + \alpha\tau E(t) \quad (2)$$

$$C_c \frac{\partial T_c}{\partial t} = \frac{T_f - T_c}{R_{cf}} + \frac{T_p - T_c}{R_{pc}} \quad (3)$$

$$C_f \left( \frac{\partial T_f}{\partial t} + \bar{u} \frac{\partial T_f}{\partial x} \right) = \frac{T_c - T_f}{R_{cf}} \quad (4)$$

All approximations of this model are not repeated. We only mention that the capacities and the heat resistances are assumed to be constant. Both heat resistances  $R_{ag}$  and  $R_{cf}$  are very small,  $R_{pg}$  is nearly equal to the heat loss resistance  $R_L$ . In the mathematical derivations, the ratios  $R_{ag}/R_L$  and  $R_{cf}/R_L$  are neglected with respect to 1. As indicated in e.g. [2], and confirmed by our own measurements with a dismantlable Philips ETC-VTF collector,  $R_{pc}$  is relatively large and the ratio  $R_{pc}/R_L$  cannot be neglected with respect to 1. The same measurements show a nearly constant value of  $R_{pc}$  for various values of the useful energy. In our approximations  $R_{pc}$  has been taken as a constant.

Introducing the Fourier transform of the time-

## NOMENCLATURE

$C$	heat capacity per $m^2$ [ $J K^{-1} m^{-2}$ ]	$Y_R, Y_I$	real and imaginary part of the complex function $\tilde{Y}(\omega)$ [ $K s$ ]
$E$	the insolation [ $W m^{-2}$ ]	$\tilde{Z}(\omega), \tilde{U}(\omega)$	parts of the generalized expression of the useful energy [ $J m^{-2}$ ]
$\hat{E}$	the Fourier transform of $E$ [ $W m^{-2} s$ ]	$Z_R, Z_I$	real and imaginary part of the complex function $\tilde{Z}(\omega)$ [ $J m^{-2}$ ].
$R$	thermal resistance per $m^2$ [ $W^{-1} K m^2$ ]	Greek symbols	
$R_L$	total heat loss resistance per $m^2$ [ $W^{-1} K m^2$ ]	$\alpha\tau$	absorptance-transmittance product
$t$	coordinate of time [s]	$\delta, \eta, \kappa$	coordinates of the Cartesian coordinate system defining the points $(Y_R/X_R, Z_R/X_R, U_R/X_R)$ or $(Y_I/X_I, Z_I/X_I, U_I/X_I)$ , Fig. 2 [ $W m^{-2} K^{-1}, -, -$ ]
$t_e$	time interval of the measurements [s]	$\omega$	Fourier variable [ $s^{-1}$ ]
$t_0$	initial time of the measurements [s]	$\omega^*$	Fourier variable, defining the minimum value of $Y_I(\omega)$ near $\omega t_e/\pi = 2$ [ $s^{-1}$ ].
$T$	the temperature of a part of the collector [K]	Subscripts	
$\hat{T}$	the Fourier transform of $T$ [ $K s$ ]	a	ambient
$u$	velocity of the fluid flow [ $m s^{-1}$ ]	c	condensator
$U_R, U_I$	real and imaginary part of the complex function $\tilde{U}(\omega)$ [ $J m^{-2}$ ]	f	fluid
$x$	space coordinate in the flow direction [m]	g	cover plate
$\tilde{X}(\omega)$	the Fourier transform of the insolation [ $J m^{-2}$ ]	p	absorber plate.
$X_R, X_I$	real and imaginary part of the complex function $\tilde{X}(\omega)$ , [ $J m^{-2}$ ]		
$\tilde{Y}(\omega)$	the Fourier transform of the difference of the fluid inlet temperature and the ambient temperature [K s]		

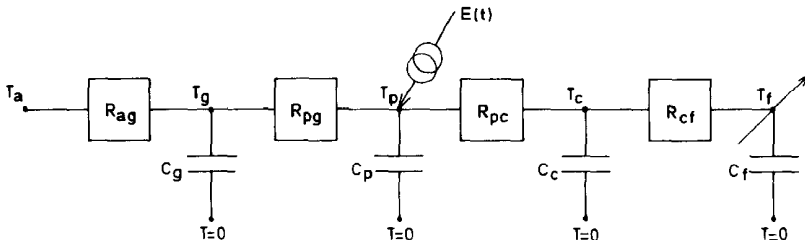


FIG. 1. The heat resistance analogue representing the collector.

dependent quantities, such as the temperature as

$$\hat{T}(x, \omega) = \int_0^{t_e} e^{-i\omega t} T(x, t) dt, \quad (5)$$

the set (1)–(4) can be transformed into the Fourier frequency domain.

By a reasoning very similar to the one for the flat plate collector [1, Appendix], the basic equation can be formulated as

$$\tilde{Z}(\omega) - R_{pc}/R_L \cdot \tilde{U}(\omega) = F'\alpha\tau \cdot \tilde{X}(\omega) - F'/R_L \cdot \tilde{Y}(\omega), \quad (6)$$

the efficiency factor being defined as

$$F' = R_L/(R_L + R_{pc}). \quad (7)$$

The functions  $\tilde{X}(\omega)$  and  $\tilde{Y}(\omega)/R_L$  can be understood as a generalization of the insolation and the heat losses, respectively. The terms of the LHS of (6) represent the useful energy, showing a series expansion with respect to  $R_{pc}/R_L$ . The relation (6) contains the functions  $\tilde{X}$ ,  $\tilde{Y}$ ,  $\tilde{Z}$  and  $\tilde{U}$  as complex functions. Taking the real and the imaginary parts, respectively, of (6), the algebraic equations suited for the test method can be derived as

$$Z_R/X_R = F'\alpha\tau - F'/R_L \cdot Y_R/X_R + R_{pc}/R_L \cdot U_R/X_R \quad (8)$$

$$Z_I/X_I = F'\alpha\tau - F'/R_L \cdot Y_I/X_I + R_{pc}/R_L \cdot U_I/X_I. \quad (9)$$

Defining a three-dimensional Cartesian coordinate

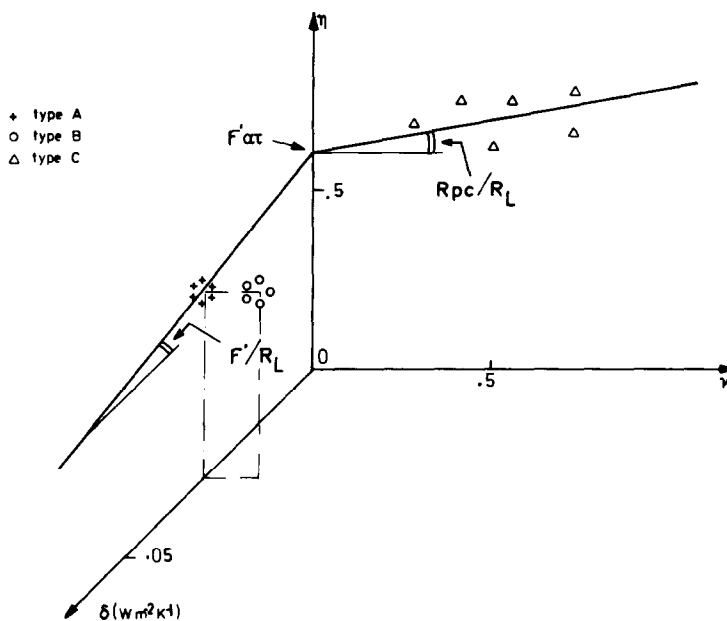


FIG. 2. The  $(\delta, \eta, \kappa)$ -space showing the selected points of the types A, B and C. The least-square approximation of the flat plane defines  $F'\alpha\tau$ ,  $F'/R_L$  and  $R_{pc}/R_L$ .

system  $(\delta, \eta, \kappa)$ , the points of, respectively,  $(\delta, \eta, \kappa) \equiv (Y_R/X_R, Z_R/X_R, U_R/X_R)$  corresponding to (8) and  $(\delta, \eta, \kappa) \equiv (Y_I/X_I, Z_I/X_I, U_I/X_I)$  corresponding to (9), can be plotted. The collector parameters have to be derived from this set of points according to the relation

$$\eta = F'\alpha\tau - F'/R_L \cdot \delta + R_{pc}/R_L \cdot \kappa. \quad (10)$$

The least-square approximation consists of a flat plane in the  $(\delta, \eta, \kappa)$ -space, shown in Fig. 2. The intersection of the  $\eta$ -axis with this plane defines the value of  $F'\alpha\tau$ . The values of  $F'/R_L$  and  $R_{pc}/R_L$  are determined by the slopes of the intersection of the plane with the  $(\delta, \eta)$ -plane and the  $(\eta, \kappa)$ -plane, respectively.

As a last remark it is mentioned that, analogously to the flat plate collectors, the functions of  $X_R, Y_R, Z_R, U_R$  and  $X_I, Y_I, Z_I, U_I$  very weakly depend on the heat capacities and the heat resistances of the collector model. Usually, they can be estimated from the collector design. The only exception forms the dependence on  $R_{pc}$ . The final value of the resistance  $R_{pc}$  follows iteratively by a repeated application of the test procedure described above.

### 3. THE TESTING OF THE PHILIPS ETC-VTR 141 COLLECTOR

The test method has been applied to a module of 19 Philips ETC-VTR 141 tubes. They were mounted with an interspace of 0.006 m above a white-painted background. Each collector tube consists of a cylindrical evacuated space, enveloped by a glass cover. Within this space a flat absorber, spectrally selective on both sides, receives the solar radiation. A heat pipe fixed at the absorber, transports the generated heat to its

condensor. Via a special clamping block the heat is collected by the circulating fluid. More details of the Philips tube may be found in ref. [3].

In each tube, the temperatures of the various parts, such as the glass envelope, the absorber, the condenser and the fluid are assumed to be constant.

Introducing a space coordinate along the header of the circulating fluid in the direction of an increasing serial number of the tubes, the behaviour of the temperatures can be approximated by continuous functions of this space variable. In this approximation the collector can be represented by the set of differential equations (1)–(4).

The model has been tested outside. In each experiment both the fluid rate and the fluid inlet temperature have been chosen equal to a constant value. Every 10 s the insolation, the ambient temperature, the fluid inlet and outlet temperature are experimentally measured and recorded on tape. Several series of experimental measurements during periods of about 2 h are made under varying weather circumstances. In the case of a stationary insolation, a time-dependent covering of the collector by a semi-transparent shield can supply the required transient conditions. Figure 3 illustrates a part of a series of measured data. It shows the special case of an insolation of a nearly perfect square-wave function, resulted from a periodic shielding on a bright day.

In order to apply the Fourier transformation, time intervals of a length of  $t_c$  beginning at the initial time  $t_0$  are defined in the series of experimental measurements. In practice, periods of  $t_c$  equal to 2000–3000 s have been chosen. The Fourier transforms of the insolation and the various temperatures, respectively, can be computed for every value of the Fourier variable  $\omega$ .

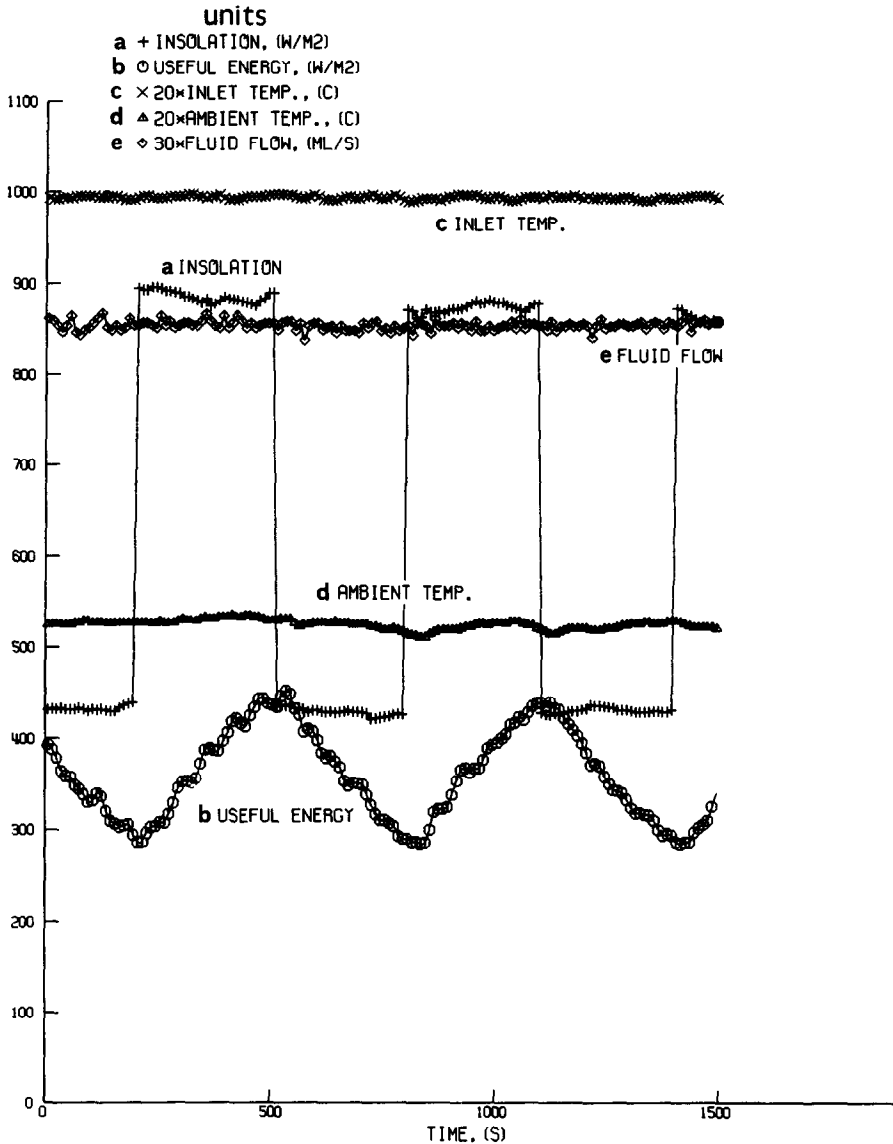


FIG. 3. Plots of the experimental measurements of, respectively, (a) the insolation, (b) the useful energy, (c) the inlet temperature, (d) the ambient temperature and (e) the fluid flow. A periodic shielding supplies the varying insolation.

Together with the heat capacities and reasonable estimates of the heat resistances, they determine the functions of  $\bar{X}$ ,  $\bar{Y}$ ,  $\bar{Z}$  and  $\bar{U}$  of (6). The computation of the real and the imaginary parts of these functions yield the required functions of  $X_R$ ,  $Y_R$ ,  $Z_R$ ,  $U_R$  and  $X_I$ ,  $Y_I$ ,  $Z_I$ ,  $U_I$  occurring in equations (8) and (9), respectively.

Analogously to the case of the flat plate collector and explained in great detail in [1], the test method is very sensitive for errors. Similar errors occurring in calculations in the frequency domain, are mentioned in literature, [4]. In fact, suitable equations of the type (8) or (9) are defined by a very selective choice of values of  $\omega$ . Insight can be obtained from the behaviour of, respectively, the functions  $X_R$ ,  $Y_R$ ,  $Z_R$ ,  $U_R$  and  $X_I$ ,  $Y_I$ ,  $Z_I$ ,  $U_I$  with respect to  $\omega$ . For a typical example, they are shown in Figs. 4 and 5.

In this paper the extensive reasoning given in [1], leading to the final selection of values of  $\omega$ , will not be repeated. We limit ourselves to a short review of the conclusions:

(i) In each time interval, in the case of the functions  $X_R$ ,  $Y_R$ ,  $Z_R$ ,  $U_R$  (Fig. 4), only the value of  $\omega$  equal to zero is selected. The corresponding point defined by  $\delta = Y_R/X_R$ ,  $\eta = Z_R/X_R$ ,  $\kappa = U_R/X_R$ , can be plotted in the  $(\delta, \eta, \kappa)$ -space and has been denoted as a point of type A, Fig. 2. As the values of both  $U_R$  and the  $\kappa$ -coordinate are nearly equal to zero, the positions of the points of type A are situated very near to the  $(\delta, \eta)$ -plane.

(ii) Considering the functions  $X_I$ ,  $Y_I$ ,  $Z_I$ ,  $U_I$  (Fig. 5), a range of values of  $\omega$  around  $\omega t_e/\pi \approx 0.75$ , the last

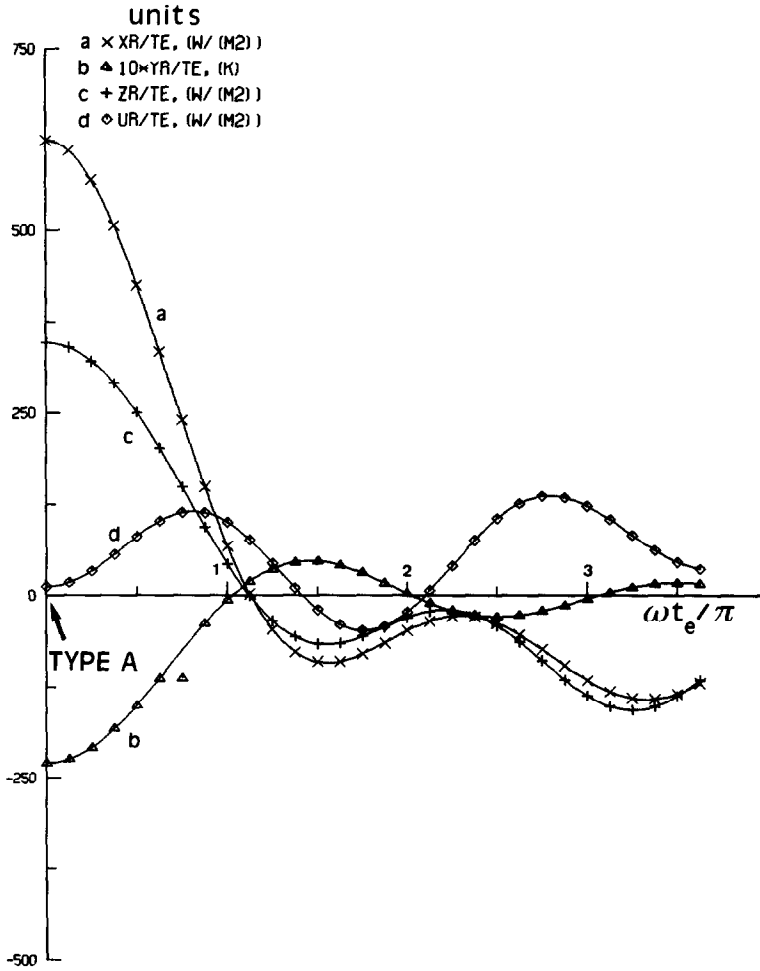


FIG. 4. The behaviour of the functions  $X_R$ ,  $Y_R$ ,  $Z_R$  and  $U_R$  with respect to the Fourier variable is shown in the curves (a), (b), (c) and (d) respectively. The points of type A are found for  $\omega = 0$ .

one defining extrema for  $X_1$ ,  $Y_1$  and  $Z_1$ , respectively is appropriate to use in the test method. In order to maximize the influence of  $R_{pe}$  in our calculations the value of  $\omega$ , defined by  $\omega t_e/\pi = 0.375$ , yielding a maximum value of  $U_1$  has been selected. The corresponding point in the  $(\delta, \eta, \kappa)$ -space has been denoted as a point of type B, Fig. 2. The point B is found a small distance outside the  $(\delta, \eta)$ -plane with the projection on the  $(\delta, \eta)$ -plane very near to that of point A.

(iii) A third value of  $\omega$  follows by considering the minimum value of  $Y_1$  near  $\omega t_e/\pi \approx 2$  in the case of the functions  $X_1$ ,  $Y_1$ ,  $Z_1$ ,  $U_1$ , Fig. 5.

This stable value of  $Y_1(\omega)$  obtained for the value of the Fourier variable  $\omega^*$ , is nearly equal to zero (Fig. 5). As explained in [1], only an appropriate equation of the type (9) results for  $\omega^*$ , if the corresponding  $X_1(\omega^*)$  is sufficiently large. As  $X_1(\omega^*)$  depends on the time interval  $t_e$ , for the given initial time  $t_0$  the behaviour of  $X_1(\omega^*)$  with respect to a variable time interval  $t_e$  has been determined (not shown in this paper).

The appropriate time intervals  $t_e$  are defined by sufficiently large extrema of this behaviour. Each of

these time intervals defines for the corresponding Fourier variable  $\omega^*$  a point of the type C in the  $(\delta, \eta, \kappa)$ -space, Fig. 2. The  $\delta$ -coordinate of the point C given by  $\delta = Y_1(\omega^*)/X_1(\omega^*)$  is nearly equal to zero. Hence, the position of the point C is found in or very near to the  $(\eta, \kappa)$ -plane.

Now we are able to consider one series of experimental data measured at a fixed fluid inlet temperature. Various time intervals can be chosen. In principle, each interval yields points of the types of A, B and C.

As indicated in Fig. 2, a cluster of points of the type A has been found near the  $(\delta, \eta)$ -plane. These points nearly coincide, because the heat losses defined by  $Y_R/R_L$ , are proportional to the nearly constant difference of the fixed fluid inlet temperature and the ambient temperature for each interval.

A cluster of points of the type B is found at a small distance outside the  $(\delta, \eta)$ -plane. The projections of the points B on the  $(\delta, \eta)$ -plane appear to coincide with the positions of the points A.

The points of the type C have in common that

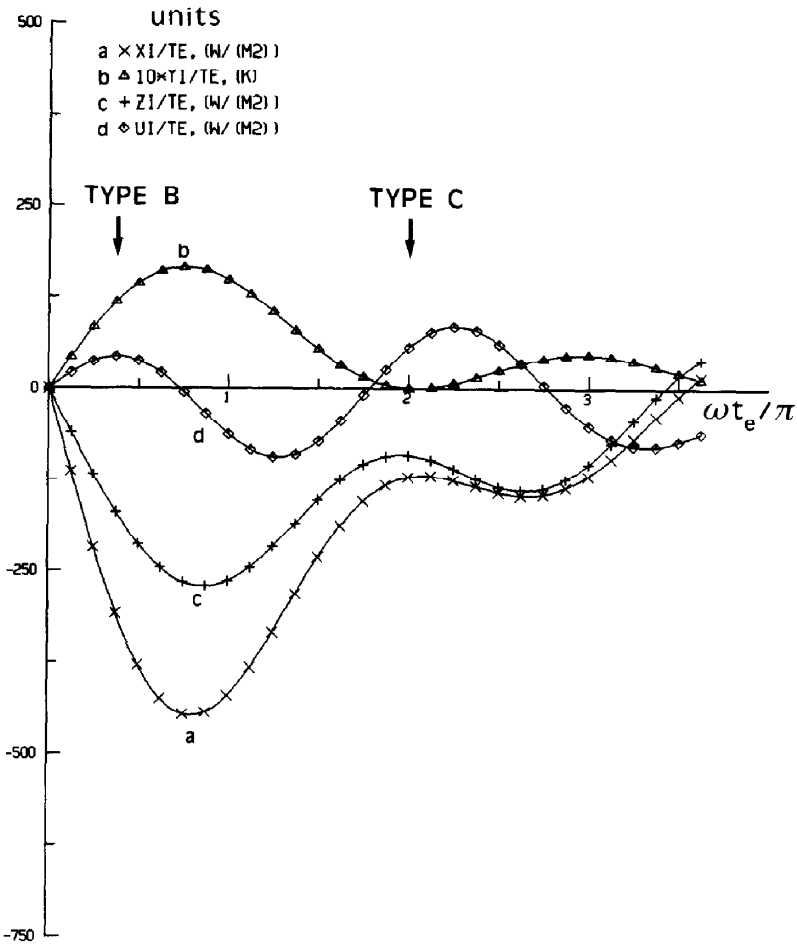


FIG. 5. The behaviour of the functions  $X_1$ ,  $Y_1$ ,  $Z_1$  and  $U_1$  with respect to the Fourier variable is shown in the curves (a), (b), (c) and (d), respectively. The points of the type B and C are found for the indicated values of  $\omega$ .

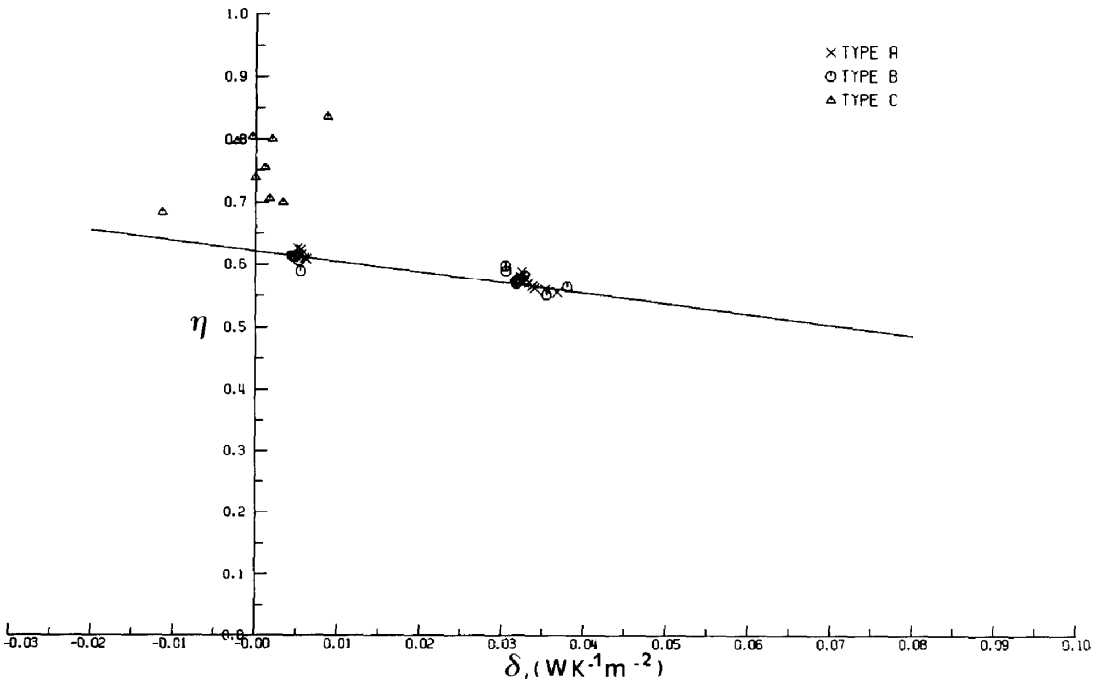


FIG. 6. The projections on the  $(\delta, \eta)$ -plane of the selected points A, B and C. Shown are the results of two series of experimental measurements with a fluid inlet temperature of 25 and 40°C, respectively. (The ambient temperature was about 20°C.)

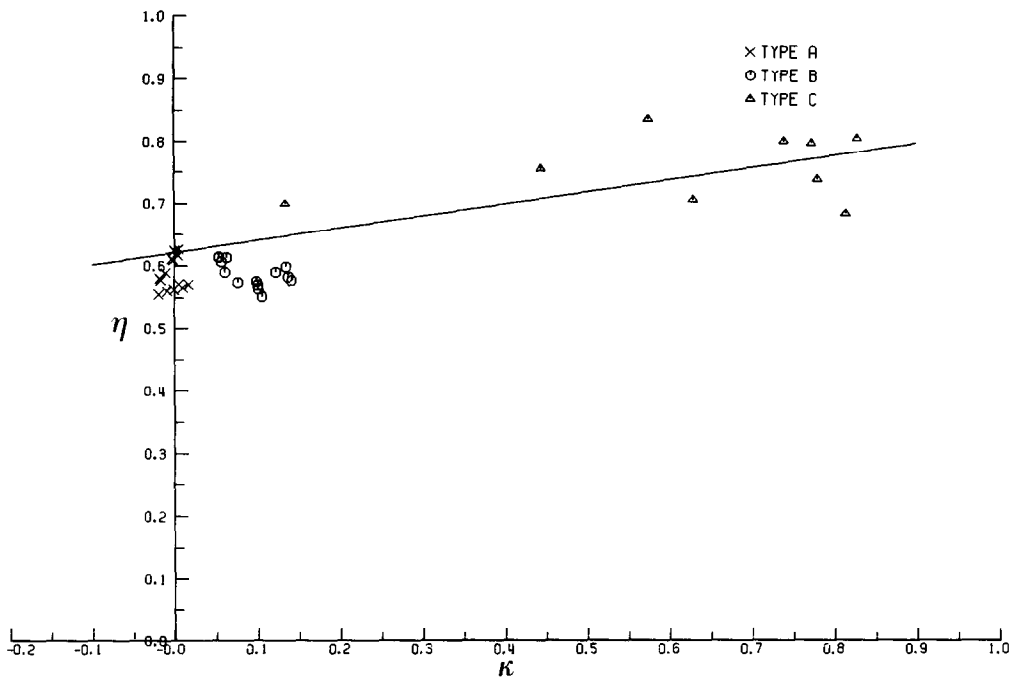


FIG. 7. The projections on the  $(\eta, \kappa)$ -plane of the same selected points considered in Fig. 6.

they are very near to the  $(\eta, \kappa)$ -plane and that the  $\eta$ -coordinate is approximately equal to  $F'\alpha\tau$ . At the other hand the size of the  $\kappa$ -coordinate seems to be unpredictable. An illustration of the various positions of the points C in the  $(\delta, \eta, \kappa)$ -space has been given in Fig. 2.

In order to obtain appropriate points of the type C experimental measurements having an insolation of slowly varying dominant periods of say 1200 s, are recommended. In that case the extremal values of  $X_1(\omega^*)$  are found to be sufficiently large for time intervals of 2000–3000 s.

Generally, the points of the types A, B and C obtained from one series of experimental data with a fixed fluid inlet temperature are not sufficient to determine an accurate least-square approximation of the collector characteristics of the heat pipe collector. A much better approximation has been obtained when a second series of data with a different fluid inlet temperature has been considered. In that case two clusters of points A nearly independent of  $R_{pc}$  are found at different positions near the  $(\delta, \eta)$ -plane. In fact these clusters of the points of type A mainly determine the line of intersection of the least-square plane with the  $(\delta, \eta)$ -plane, defining the collector characteristics  $F'\alpha\tau$  and  $F'/R_L$ . Next, the iterative solution of  $R_{pc}/R_L$  is straightforward.

Various series of experiments with a different fluid inlet temperature have been made with the Philips module. Figures 6 and 7 show the projection of the points A, B and C on respectively the  $(\delta, \eta)$ -plane and the  $(\eta, \kappa)$ -plane, obtained from 14 time intervals chosen

from two series of data with a fluid inlet temperature of 25° and 40°C, respectively. The least-square approximation leads to the values of  $F'\alpha\tau = 0.621 \pm 0.013$ ,  $F'/R_L = 1.66 \pm 0.47 \text{ W K}^{-1} \text{ m}^{-2}$  and  $R_{pc}/R_L = 0.19 \pm 0.03$ . The approximation has been refined by the extension to 31 time intervals taken from five series with different fluid inlet temperatures. In that case the values of  $F'\alpha\tau = 0.616 \pm 0.008$ ,  $F'/R_L = 1.67 \pm 0.25 \text{ W K}^{-1} \text{ m}^{-2}$  and  $R_{pc}/R_L = 0.16 \pm 0.02$  are found. Characteristic collector parameters are derived to be  $\alpha\tau = 0.71$ ,  $R_L = 0.52 \text{ W}^{-1} \text{ K m}^2$  and  $F' = 0.87$ .

#### 4. CONCLUSIONS

The testing of the evacuated tubular collector with a heat pipe using the method described in this paper, yields accurate approximations of the absorptance-transmittance product, the heat loss resistance and the efficiency factor; caused by errors, the method can be applied for very selected choices of the Fourier variable.

Experimental measurements with a different fixed fluid inlet temperature have to be made. Both a value near the ambient temperature and a value much higher than the ambient temperature appear to be favourable choices of the fluid inlet temperature.

*Acknowledgements*—The author wishes to thank J. Havinga and A. J. Lutz. They constructed the collector test installation and supplied most of the experimental measurements used in ref. [1] and this paper.

## REFERENCES

1. W. Kamminga, Experiences of a solar collector test method using Fourier transfer functions, *Int. J. Heat Mass Transfer* **28**, 1393–1404 (1985).
2. A. A. Green, Computer model of the CEC5 Philips evacuated tubular solar collector, Report 987/SEU 378, Department of Mechanical Engineering, University College, Cardiff (1983).
3. H. Bloem, J. C. de Grijs and R. L. C. de Vaan, Evacuated tubular collector with two-phase heat transfer into the system, *Proc. ISES Solar World Forum*, Brighton 1981, Vol. 1, pp. 176–180. Pergamon Press, Oxford (1982).
4. R. Klüppel, A. de Nobrega, R. Sizmann and W. Schölkopf, Measurement of characteristic solar collector parameters in transient operation, *Proc. ISES Solar World Congress*, Perth 1983, Vol. 2, pp. 874–878. Pergamon Press, Oxford (1984).

ESSAI D'UN COLLECTEUR TUBULAIRE D'EVACUATION MUNI D'UN CALODUC,  
A PARTIR DU DOMAINE DE FREQUENCE DE FOURIER

**Résumé**—On étudie un collecteur tubulaire muni d'un caloduc avec une isolation thermique variable. Basé sur un bilan de chaleur défini dans un domaine de fréquence de Fourier, un système d'équations peut être formulé, correspondant aux valeurs sélectives de la variable de Fourier. Les paramètres principaux du collecteur tels que le produit absorptance-transmittance, la résistance de fuite de chaleur et le facteur d'efficacité, résultent d'une approximation de moindre carré. Enfin deux séries de mesures avec des températures d'entrée de fluide différentes sont utilisées.

EIN TEST-VERFAHREN FÜR EINEN VAKUUM-'HEAT-PIPE'-KOLLEKTOR UNTER  
VERWENDUNG DES FOURIER'SCHEN FREQUENZ-BEREICHES

**Zusammenfassung**—Beschrieben wird eine 'Outdoor'-Methode zum Test eines evakuierten 'Heat-Pipe'-Kollektors bei wechselnder Einstrahlung. Aufbauend auf der Wärmebilanz des Kollektors, beschrieben im Fourier'schen Frequenzbereich, wird entsprechend den ausgewählten Werten der Fourier-Variablen ein System von Gleichungen formuliert. Die wichtigsten Kollektorparameter, wie das Absorptions-Transmissions-Produkt, die Güte der Wärmedämmung und der Wirkungsgrad folgen aus einer Berechnung der kleinsten Fehlerquadrate. Schließlich sind noch zwei Serien experimenteller Messungen mit verschiedenen Einlaßtemperaturen des Fluids erforderlich.

ИСПЫТАНИЕ ГЕРМЕТИЧНОГО ТРУБЧАТОГО КОЛЛЕКТОРА С ТЕПЛОЙ  
ТРУБОЙ С ПОМОЩЬЮ ЧАСТОТНОГО МЕТОДА

**Аннотация**—Описан метод испытаний вне помещения герметичного трубчатого коллектора с тепловой трубой и различной тепловой изоляцией. Базируясь на частотном представлении теплового баланса в коллекторе, получена система уравнений, в которых соответствующим образом подобраны коэффициенты Фурье-преобразования. Из среднеквадратичных аппроксимаций могут быть определены основные параметры коллектора, такие как поглощательно-пропускная способность, сопротивление тепловых потерь и коэффициент полезного действия. Для этого необходимо проведение по крайней мере двух серий экспериментов с различными температурами жидкости на входе.